Journal of Inflammation Research

Dovepress
Taylor & Francis Group

Open Access Full Text Article

ORIGINAL RESEARCH

Preliminary Retrospective Analysis of X-Ray, CT, and MRI Imaging Features of Brucellar Spondylodiscitis Diagnosis

Ying Pu[1,*], Xu-Wen Fu[2,*], Min Qi[1], Jia-Lu Wei[1], Qiu-Lan Shan[1], Wei Gan[1], Xin-Hua Cun[3], Xiang Li[1]

[1]Department of Radiology, Kunming Third People's Hospital/Yunnan Clinical Medical Center for Infectious Diseases, Kunming, Yunnan, People's Republic of China; [2]Department of Pharmacy, Kunming Third People's Hospital/Yunnan Clinical Medical Center for Infectious Diseases, Kunming, Yunnan, People's Republic of China; [3]Department of Orthopaedics, Kunming Third People's Hospital/Yunnan Clinical Medical Center for Infectious Diseases, Kunming, Yunnan, People's Republic of China

*These authors contributed equally to this work

Correspondence: Xiang Li, Department of Radiology, Kunming Third People's Hospital/Yunnan Clinical Medical Center for Infectious Diseases, 319 Wujing Road, Guandu District, Kunming, Yunnan, 650041, People's Republic of China, Tel +86-18108857532, Email li_xiang115@126.com; Xin-Hua Cun, Department of Orthopaedics, Kunming Third People's Hospital/Yunnan Clinical Medical Center for Infectious Diseases, 319 Wujing Road, Guandu District, Kunming, Yunnan, People's Republic of China, Email xinhuacun_cun6@21cn.com

Objective: To explore the X-ray, CT, and MRI imaging features of Brucellar spondylodiscitis (BS) across different stages and evaluate their diagnostic value.

Methods: Retrospective analysis of imaging features in 137 BS patients (early stage: 40; advanced: 52; recovery: 45) classified by the 2023 Chinese Medical Association Consensus. Diagnostic performances of X-ray, CT, and MRI were compared.

Results: Lumbar involvement predominated (98.5%), with 73.7% single-segment cases. X-ray missed 90% of early-stage BS but detected intervertebral stenosis/bone destruction better in advanced/recovery stages ($P<0.05$). CT excelled in identifying bone destruction (83.9%), sequestration (5.1%), and fractures (6.6%). MRI detected granulomas (85.4%) and abscesses (3.6%) effectively, especially granulomas in advanced-stage ($p < 0.05$, compared with early stage and recovery stage). CT+MRI synergistically improved staging accuracy for early/advanced BS.

Conclusion: CT and MRI are critical for BS staging, with combined use recommended to minimize misdiagnosis and guide treatment.

Keywords: brucellosis, spondylitis, magnetic resonance imaging, diagnostic imaging

Background

Brucellosis, an infectious zoonotic disease caused by brucella infection, has become a global public health problem.[1] According to a World Health Organisation (WHO) report, over 500,000 cases of brucellosis are reported annually across countries and regions worldwide.[2] In China, the incidence of brucellosis has increased over the years, with an overall rate of 3/100,000.[3] The incidence of this disease is increased in areas with developed animal husbandry in northern China compared with that in southern China due to the more frequent contact with livestock such as cattle and sheep.[4] However, the incidence in southern China, especially in Yunnan province, has increased significantly in recent years.[5] Yunnan province is located on the southwestern border of China, and the epidemic status of brucellosis in this economically underdeveloped area is characterized by sporadic outbreak, with a wide and complex spatial and temporal distribution, which increases the difficulty of prevention and diagnosis of this disease.[6]

Brucellosis can affect multiple organs and systems in the body, particularly the bones and joints, with an incidence rate of 2%-77%.[7,8] Brucellar spondylodiscitis (BS) is one of the most common manifestations in cases with bone and joint system involvement. The diagnosis of BS requires a combination of epidemiological background, clinical manifestations, laboratory tests, and imaging findings. However, the diagnosis and differential diagnosis of BS is significantly

Received: 16 June 2025
Accepted: 21 November 2025
Published: 3 December 2025

challenged by the lack of specific clinical symptoms and the high similarity in imaging findings with diseases such as intervertebral disc herniation and tuberculous spondylitis.[9] BS is characterized by a progressive inflammatory response triggered by Brucella invasion. After the bacterium spreads hematogenously to the spine, it proliferates in the vertebral endplate and intervertebral disc, activating macrophages and neutrophils to release pro-inflammatory cytokines (eg, TNF-α, IL-6), which induce early pathological changes of inflammatory edema, congestion, and microvascular hyperplasia in the vertebral marrow and surrounding soft tissues. As the disease progresses, sustained inflammation drives bone resorption by osteoclasts and concurrent repair by osteoblasts, leading to mixed lesions of bone destruction and sclerosis, while persistent inflammatory infiltration can further form paravertebral granulomas or rare abscesses. In the early stage of BS when this disease is mainly characterized by inflammation, edema, and congestion, leading to indistinct imaging features and consequently missed diagnosis or misdiagnosis.

In the Experts Consensus on Imaging Diagnosis of BS issued by the Chinese Medical Association in 2023,[10] BS is classified into the early, advanced, and recovery stages, and the corresponding X-ray, CT, and MRI imaging features are summarized. The manifestations of BS mainly include inflammation and edema in the early stage, concurrent bone destruction and repair in the advanced stage, and bone sclerosis in the recovery stage. This classification of BS is highly valuable for clinical management: in the early stage, when imaging is dominated by subtle inflammatory changes, timely anti-infection treatment can effectively prevent bone destruction; in the advanced stage, where bone destruction and repair coexist, the classification guides clinicians to evaluate the extent of bone damage and soft tissue involvement to decide whether anti-infection therapy alone or combined with surgical intervention is needed; in the recovery stage, characterized by osteosclerosis, the classification helps monitor treatment response and adjust therapeutic courses by tracking the regression of inflammatory lesions and progression of sclerosis. Previous studies have highlighted the crucial role of imaging modalities in the differential diagnosis of BS. X-ray, due to its limited sensitivity in detecting early bone changes, often results in missed diagnoses in the initial stages of BS.[10] CT has been widely recognized for its superior ability to detect bone destruction and sequestra, making it valuable for differentiating BS from other infectious spondylodiscitis with similar bone involvement.[11] MRI, with its high soft tissue contrast, excels in identifying early inflammatory changes and granulomas, which are key features distinguishing BS from pyogenic or tuberculous spondylodiscitis.[12] MRI's high soft tissue resolution—especially on fat-suppressed T2WI and T1WI sequences—can sensitively detect early bone marrow edema and subtle paravertebral inflammatory infiltration in the absence of obvious bone destruction. Additionally, MRI can clearly distinguish inflammatory granulomas from abscesses, enabling early identification of inflammatory progression that is critical for timely intervention. The combined use of CT and MRI has increasingly been advocated to provide a comprehensive assessment, enhancing diagnostic accuracy and aiding in the precise staging and treatment planning of BS.[13] However, the specific features and clinical application values of each imaging examination in different stages of disease have not been addressed in this consensus.

In order to fill this research gap, imaging data of 137 patients with newly diagnosed BS were analyzed, and the diagnostic performances of X-ray, CT and MRI in the early, advanced and recovery stages of this disease were compared in the present study to explore the advantages and disadvantages of each imaging examination. This foundational study was designed to improve the accuracy of BS diagnosis, explore the best combination of imaging examinations, and reduce missed diagnosis and misdiagnosis to provide theoretical and data groundwork for future large-scale multi-center studies that further validate the optimal imaging strategy for BS staging and treatment evaluation.

Materials and Methods

Ethical Approval and Informed Consent

This study was conducted strictly following the ethical requirements of medical studies in the Helsinki Declaration (2013 Revision) and approved by the Ethics Committee of Kunming Third People's Hospital (Ethical Approval No.: KSLL20230711001-01). All participants signed a written informed consent before entering the study. For patients who could not provide written consent (such as minors or under special circumstances), their legal representatives signed on their behalf. Special circumstances include: ① patients who were bed-ridden due to spinal surgery could not sign the informed consent form, which was signed by their legal representatives; ② Some elderly patients in pastoral areas who

could not sign the informed consent because of their educational level, which was signed by their legal representatives. Participants were informed of the following contents in the informed consent form: the objective, procedure, and possible risks and benefits of the study; principles of personal privacy and data confidentiality; and the right to participate voluntarily and the right to withdraw from study at any time. Data from all subjects were recorded anonymously, used by study personnel only, and encrypted to ensure data security.

Study Subjects

Patients diagnosed with BS in Kunming Third People's Hospital between Jan. 2021 and Aug. 2024 were retrospectively analyzed in this study. Inclusion criteria included patients who met the diagnostic criteria for brucellosis in the Chinese Health Industry Standard - Diagnosis for Brucellosis (WS-269-2019) and the imaging diagnostic criteria for BS in the Experts consensus on imaging diagnosis of BS (2023) issued by the Chinese Medical Association. The calculation of sample size in this study was based on the formula: $n=Z^2*p*(1-p)/d^2$, where Z = 1.96 (95% confidence level), p = 0.5 (assumed incidence), and d = 0.1 (allowable error). These values were introduced in the formula and n = 96.06 was obtained, and consequently a sample size of at least 96 patients was required theoretically. Additionally, the G*Power (version 3.1.9.7) analysis was performed to further verify the statistical power: with an effect size of 0.3 (medium effect, referenced from similar imaging diagnostic studies), $\alpha=0.05$, and power $(1-\beta)=0.8$, the calculated required sample size was 89, which was smaller than our actual sample size of 137. This confirmed that the sample size of this study was sufficient to detect the intended differences in diagnostic performance among imaging modalities.

Inclusion and Exclusion Criteria

Inclusion criteria included patients (1) with BS confirmed by pathologic, pathogenic or clinical diagnosis; (2) with complete X-ray, CT, and MRI imaging data and the X-ray, CT, and MRI examinations were conducted within 72 hours after the definite diagnosis of BS and before initiating any systemic anti-infection or surgical treatment; and (3) who were diagnosed for the first time without previous systemic anti-infection or surgical treatment. Exclusion criteria included patients (1) with no spinal involvement; (2) with incomplete clinical and imaging data; (3) complicated with other diseases that affect the spine, such as spinal tuberculosis, pyogenic spondylitis, and tumors; (4) with serious systemic diseases or other comorbidities, such as multiple myeloma and bone metabolism disorders, that may affect the imaging evaluation; (5) who were readmitted or had already received treatment (such as systemic anti-infection, surgical or anti-tuberculosis treatment); and (6) who did not provide informed consent or were not approved by the ethics committee.

Definite Diagnosis of Brucellosis

The diagnosis of brucellosis was based on the Chinese Health Industry Standard - Diagnosis for Brucellosis (WS-269-2019) and the following criteria:

Epidemiological History

A history of close contact with livestock such as cattle, sheep, and pigs, or contact with contaminated animal products such as raw milk, raw meat, or cheese that has not been subjected to high temperature treatment.

Clinical Manifestations

The presence of typical symptoms of brucellosis, including fever, night sweats, fatigue, joint or muscle pain, and corresponding symptoms of spinal involvement (such as lower back pain).

Laboratory Testing

Pathogenic testing: Isolation and culture of Brucella from blood or other body fluids;

Serological testing: An increased titer of antibody against Brucella by using common testing methods such as the standard agglutination test (SAT) and the serum tube agglutination test.

Molecular Testing: Presence of Brucella DNA Detected by PCR

Definite diagnosis of brucellosis was confirmed by microbiological evidence as the primary criterion (positive Brucella culture from vertebral bone, intervertebral disc tissue, or paravertebral abscess aspirate). For patients without obtainable microbiological samples (eg, contraindications to invasive biopsy), diagnosis relied on a combination of positive serological testing (standard agglutination test titer ≥1:160), typical clinical manifestations (persistent fever, lumbosacral pain, contact history with infected animals), characteristic imaging features, and consistent response to targeted anti-Brucella therapy confirmed by 6-month clinical follow-up.

Imaging Examination

All imaging examinations strictly followed standardized protocols to ensure uniformity. The spinal X-ray was taken using the modern X-ray equipment [United Imaging (Shanghai, China), model: uDR780], with a tube voltage of 75kV for posteroanterior view and 85kV for lateral view, and a tube current of 500mA. Images were consistently acquired in posteroanterior and lateral positions for all patients; CT examination was performed using the modern CT equipment [United Imaging (Shanghai, China), model: uCT960], with a tube voltage of 120kV and automatic tube current modulation. The CT slice thickness was 5mm, and the reconstructed slice thickness was 0.55mm. Multiplanar reconstruction (MPR) in sagittal and coronal planes was mandatory for all cases to standardize structural assessment; MRI examination was performed using the modern MR equipment [United Imaging (Shanghai, China), model: uMR780], and imaging sequences included sagittal T1WI, T2WI, fat-suppressed T2WI, and transverse T2WI. TR of 500ms, TE of 9ms, and slice thickness of 4mm were used for T1WI sequence, TR of 2500ms, TE of 100ms, and slice thickness of 4mm were used for T2WI sequence, and TR of 2400ms, TE of 90ms, and slice thickness of 4mm were used for fat-suppressed T2WI. Gadopentetate dimeglumine (0.1 mmol/kg) was intravenously injected uniformly for patients with normal renal function (estimated glomerular filtration rate ≥60 mL/min/1.73m^2). 8 patients with renal insufficiency (eGFR <60 mL/min/1.73m^2) underwent non-contrast MRI. The Diffusion-Weighted Imaging (DWI) and Apparent Diffusion Coefficient (ADC) sequences were not applied to all patients as this study focused on conventional modalities (X-ray, CT, basic MRI sequences) aligned with routine clinical practice in resource-limited regions, where advanced sequences were not universally accessible. Imaging data of all included patients were systematically reviewed and analyzed, and the findings of X-ray, CT, and MRI examinations for BS in the early, advanced, and recovery stages were summarized. Changes in intervertebral spaces and endplates were evaluated using X-ray examination, bone destruction and sequestration were observed using CT, and bone marrow edema, paravertebral granuloma and abscess were identified using MRI. Based on existing literature,[11] classification and summarization of the imaging features of different stages of BS were emphasized to provide a basis for the staging of this disease.

Image Analysis

The images were downloaded from the PACS of the hospital, and the X-ray, CT and MRI images of the patients were read using the Radiant DICOM Viewer (Poland) to analyze the imaging findings. X-ray was used to observe the presence of vertebral bone destruction, intervertebral space stenosis, vertebral endplate destruction, osteosclerosis, and sequestrum of lesions, and bone destruction of at least 30% of bone mass loss is usually required to be detected;[12] lumbar CT was used to observe the sites of bone destruction. Specifically, the involvement of the anterior vertebral column and the middle vertebral column was observed in the ventral-dorsal direction, and the vertebral body-centered or the intervertebral disc-centered bone destruction, the presence of sequestration in the bone destruction lesions, and the presence of compression fractures were observed in the cranial-caudal direction; and vertebral MRI was used to observe the T1WI, T2WI and fat-suppressed T2WI signals of bone destruction and bone around these lesions, as well as granulomas on both sides of the affected vertebrae and under the posterior and anterior longitudinal ligaments, and psoas abscess. The T2WI signal on the affected vertebra, indicating bone marrow edema, and mild paravertebral soft tissue edema on MRI images, which were shown as high signals on fat-suppressed T2WI sequences. A figure to show a sample of the image analysis performed using Radiant viewer is presented in Figure 1. Non-contrast patients accounted for only 5.8% (8/137) of the total sample and no significant difference in diagnostic accuracy of MRI for key features (granuloma, edema) between

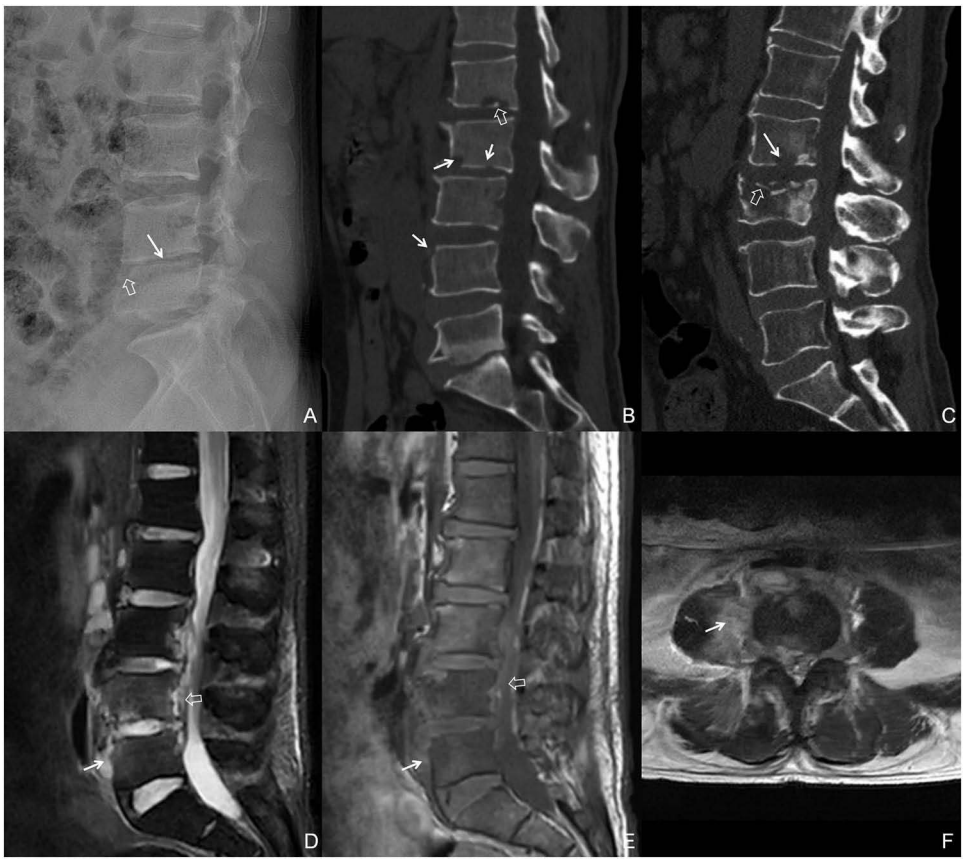

Figure 1 (A) sample of the image analysis performed using Radiant viewer. Male, 32 years old. The lateral X-ray of the lumbar spine showed stenosis of the intervertebral space between lumbar vertebrae 4 and 5 (solid white arrow), and bone destruction at the anterior upper edge of the fifth lumbar vertebra (hollow white arrow) (**A**); Male, 52 years old. Sagittal CT reconstruction of the lumbar vertebrae indicated that bone destruction of the lumbar vertebrae simultaneously involved the anterior and middle columns of the spine (solid white arrows). Stenosis of the L5-S1 intervertebral space, worm-eroded bone destruction of the endplates of the fifth lumbar vertebra and the first sacral vertebra, and hardening of the surrounding bone. Punctate high-density dead bone (hollow white arrow) within the bone destruction under the endplate of the lower edge of the first lumbar vertebra (**B**); Male, 56 years old. Sagittal CT reconstruction of the lumbar vertebrae indicated multiple bone destruction in the second and third lumbar vertebrae (solid white arrows), bone interruption of the endplate at the upper edge of the third lumbar vertebrae, and compression fracture of the third lumbar vertebrae (hollow white arrows) (**C**); Male, 64 years old. The sagittal position of the fat suppression sequence on MRI T2WI indicated high signals within the 3rd, 4th, and 5th lumbar vertebrae. Granulomas under the anterior longitudinal ligament (solid white arrow) and under the posterior longitudinal ligament (hollow white arrow) showed slightly high signals (**D**); MRI T1WI sagittal position indicated low signal within the 4th and 5th lumbar vertebrae, while granulomas under the anterior longitudinal ligament of the vertebral body (solid white arrow) and under the posterior longitudinal ligament of the vertebral body (hollow white arrow) showed equal-slightly high signal (**E**); The transverse section of the fat suppression sequence on MRI T2WI showed high-signal granulomas under the anterior longitudinal ligament and posterior longitudinal ligament, as well as a high-signal abscess in the right psoas major muscle (solid white arrow) (**F**).

contrast and non-contrast subgroups, indicating minimal impact on overall results. Blind reading was conducted by two radiologists with intermediate and above titles who have been engaged in the imaging diagnosis of infectious diseases for many years. If disagreement in the interpretation occurred between the two radiologists, a third radiologist was asked to read the images to reach a consensus conclusion after discussion. Among the 137 patients' imaging data, disagreement occurred in 12 cases (accounting for 8.76% of the total), mainly involving the identification of subtle bone destruction on CT (5 cases) and the differentiation of paravertebral granulomas from mild edema on MRI (7 cases). All 12 cases reached a consensus after consultation with a third senior radiologist. The inter-observer agreement was evaluated using Kappa coefficient (κ). The results showed that the overall inter-observer agreement for radiological findings was good (κ=0.782, 95% CI: 0.714–0.850, $p < 0.001$).

Definition of BS Stages

According to the aforementioned Experts consensus, BS was classified into the early stage, the advanced stage, and the recovery stage. The specific definitions were described below.

The Early Stage

The pathological features mainly included inflammatory edema and congestion, with no obvious bone destruction;

The imaging findings included no obvious abnormalities with occasional mild intervertebral space stenosis on X-ray images; no obvious bone destruction with only a small amount of slight density changes under the endplates on CT images; and high T2WI signal on the affected vertebra, and mild paravertebral soft tissue edema on MRI images.

The Advanced Stage

The pathological features included coexistence of bone destruction and repair, and further expansion of inflammation.

The imaging findings included obvious intervertebral space stenosis, blurred edges of the vertebral body, and visible vertebral destruction on X-ray images; obvious intervertebral disc-centered bone destruction, possibly accompanied with sequestration on CT images; and low T1WI signals and high T2WI signals on the affected vertebra, a high detection rate of granulomas and abscesses, and significant changes in the soft tissue adjacent to the affected vertebra.

The Recovery Stage

The pathological features included predominant bone repair, with an increased range of osteosclerosis.

The imaging findings included continuous intervertebral space stenosis, and obvious osteosclerosis under the endplate on X-ray images; osteosclerosis with an extent higher than that of bone destruction, and a gradually decreased mount of dead bones on CT images; and weakened signal intensity of the lesions, and significantly reduced or disappeared soft tissue granulomas and edema on MRI images.

Statistical Analysis

Data were analyzed using SPSS 26.0. Measurement data were tested for normality. Measurement data with normal distribution were presented as mean ± standard deviation $(\bar{x} \pm s)$, and univariate analysis of variance was used for the comparison of the mean values across multiple groups, and those without normal distribution were presented as the median (interquartile range) [M (Q1, Q3)], and Mann–Whitney *U*-test was used for comparison of the differences between the two groups. Differences with p values of <0.05 were considered statistically significant; enumeration data were presented as frequency (percentage), and chi-square test was used for the comparison of the differences. Differences with p values of <0.05 were considered statistically significant. Chi-square test was used for paired comparison across multiple groups, and the p values were adjusted by Bonferroni method.

Results

General Data

In this study, 137 patients with complete clinical data and X-ray, CT and MRI imaging data were finally included, including 106 males (77.4%) and 31 females (22.6%). 137 patients were classified into the early stage, advanced stage and recovery stage, with 40 patients (29.2%) in the early stage, 52 (38.0%) in the advanced stage and 45 (32.8%) in the recovery stage. No statistically significant differences in age and sex ratio were noted across patients in the early, advanced, and recovery stages (p > 0.05 for all comparisons) (Table 1).

Table 1 Sex and Age of Patients with BS in Different Stages

	The Early Stage(n=40)	The Advanced Stage(n=52)	The Recovery Stage(n=45)	χ^2/F	p
Male(frequency/percentage)	33 (82.5%)	39 (75.0%)	34 (75.6%)	0.853	0.635*
Age(years)	56.43±9.80	56.85±11.12	57.71±12.32	0.149	0.862#

Note: *chi-square test; #univariate analysis of variance.

Imaging Data

X-Ray Findings

Among the 137 patients with BS, intervertebral space stenosis was observed in 72 (52.6%) patients and bone destruction in 62 (45.3%) patients. In the 40 patients with early-stage BS, 36 (90.0%) patients were normal or misdiagnosed, and only 4 (10.0%) patients showed abnormalities. The abnormalities included intervertebral space stenosis in 3 (7.5%) patients and slight bone destruction under the vertebral endplate in 2 (5.0%) patients. In the 52 patients with advanced disease, 4 (7.7%) patients were misdiagnosed, and 48 (92.3%) had abnormalities, of which intervertebral space stenosis was observed in 35 (67.3%) patients and bone destruction under the vertebral endplate was observed in 38 (73.1%) patients. In the 45 patients in the recovery stage, 7 (15.6%) patients were misdiagnosed, and 33 (73.3%) patients had abnormalities, of which intervertebral space stenosis was observed in 34 (75.6%) patients and bone destruction under the vertebral endplate was observed in 22 (48.9%) patients. There was a statistically significant difference in the incidence of intervertebral space stenosis between the early and advanced stages, and between the early and recovery stages (P=0.000), and there was also a statistically significant difference in the incidence of bone destruction between the early and advanced stages, the early and recovery stages, and the advanced and recovery stages (p = 0.000) (Table 2).

Table 2 Imaging Findings of BS Patients in the Early, Advanced, and Recovery Stages

		Overall (n=137)	Early Stage (n=40)	Advanced Stage (n=52)	Recovery Stage (n=45)	χ^2	p
Segment involvement							
	Single	101(73.7%)	31(77.5%)	38(73.1%)	32(71.1%)	0.464	0.793*
	Multiple	36(26.3%)	9(22.5%)	14(26.9%)	13(28.9%)	0.464	0.793*
Location							
	Cervical	1(0.7%)	0(0.0%)	0(0.0%)	1(2.2%)	4.701	0.583*
	Thoracic	8(5.8%)	1(2.5%)	4(7.7%)	3(6.7%)	4.701	0.583*
	Lumbar	135(98.5%)	40(100.0%)	51(98.1%)	44(97.8%)	4.701	0.583*
	Sacral	22(16.1%)	4(10.0%)	8(15.4%)	10(22.2%)	4.701	0.583*
X-ray							
	Intervertebral space stenosis	72(52.6%)	3(7.5%)	35(67.3%)	34(75.6%)	46.650	0.000*
	Bone destruction	62(45.3%)	2(5.0%)	38(73.1%)	22(48.9%)	42.650	0.000*
CT							
	Anterior column bone destruction	20(14.6%)	8(20.0%)	3(5.8%)	9(20.0%)	3.852	0.426*
	Middle column bone destruction	2(1.5%)	1(2.5%)	1(1.9%)	0(0.0%)	3.852	0.426*
	Anterior + middle column bone destruction	115(83.9%)	31(77.5%)	48(92.3%)	36(80.0%)	3.852	0.426*
	Vertebral body-centered bone destruction	0(0.0%)	0(0.0%)	0(0.0%)	0(0.0%)	NA	NA
	Intervertebral disc-centered bone destruction	137 (100.0%)	40(100.0%)	52(100.0%)	45(100.0%)	NA	NA
	Sequestration	7(5.1%)	0(0.0%)	6(11.5%)	1(2.2%)	7.360	0.025*
	Compression fracture	9(6.6%)	0(0.0%)	5(9.6%)	4(8.9%)	3.993	0.136*
	Spondylolisthesis	9(6.6%)	0(0.0%)	4(7.7%)	5(11.1%)	4.429	0.109*
MRI							
	Granuloma on both sides of the affected vertebra	117(85.4%)	32(80.0%)	51(98.1%)	34(75.6%)	11.136	0.004*
	Granuloma under anterior longitudinal ligament	116(84.7%)	35(87.5%)	49(94.2%)	32(71.1%)	10.283	0.006*
	Granuloma under posterior longitudinal ligament	54(39.4%)	17(42.5%)	25(48.1%)	12(26.7%)	4.856	0.088*
	Psoas abscess	5 (3.6%)	1(2.5%)	4(7.7%)	0(0.0%)	4.272	0.118*

Note: *chi-square test.

Abbreviations: CT, Computed Tomography; MRI, Magnetic Resonance Imaging.

https://doi.org/10.2147/JIR.S545126

CT Findings

Among the 137 patients with BS, 20 (14.6%) had anterior vertebral column bone destruction, 2 (1.5%) had middle vertebral column bone destruction, and 115 (83.9%) had anterior and middle vertebral column bone destruction, all of which were intervertebral disc-centered. In the 40 patients with early-stage BS, 8 (20.0%) had anterior vertebral column bone destruction, 1 (2.5%) had middle vertebral column bone destruction, and 31 (77.5%) had anterior and middle vertebral column bone destruction; in the 52 patients with advanced diseases, 3 (5.8%) had anterior vertebral column bone destruction, 1 (1.9%) had middle vertebral column bone destruction, and 48 (92.3%) had anterior and middle vertebral column bone destruction; and in the 45 patients with BS in the recovery stage, 9 (20.0%) had anterior vertebral column bone destruction, and 36 (80.0%) had anterior and middle vertebral column bone destruction. No significant differences were noted in the ratios of vertebral bone destruction observed in the cranial-caudal direction and the ventral-dorsal direction ($p > 0.05$). Moreover, among the 137 patients with BS, 7 (5.1%) had sequestrum in bone destruction, 9 (6.6%) had vertebral compression fractures, and 9 (6.6%) had spondylolisthesis. No significant differences in the proportions of sequestrum in bone destruction, vertebral compression fracture, and spondylolisthesis were observed across patients in different stages ($P>0.05$) (Table 2).

MRI Findings

The area of bone destruction showed low signal shadows in the T1WI and high T2WI sequences, and high signals in the fat-suppressed T2WI sequence. The surrounding area of bone destruction showed low signals in the T1WI sequence, and marrow edema. For T2WI sequence, high, moderate, and low signals were observed in some patients. The paravertebral granulomas showed slightly low signals in T1WI and slightly marrow edema. Abscesses showed low signals in T1WI and high signals in T2WI, and high signals in the fat-suppressed T2WI sequence. Among the 137 patients with BS, 117 (85.4%) had granulomas on both sides of the affected vertebrae, 116 (84.7%) had granulomas under the anterior longitudinal ligament, 54 (39.4%) had granulomas under the posterior longitudinal ligament, and 5 (3.6%) had psoas abscess. In the 40 patients with early-stage diseases, 32 (80.0%) had granulomas on both sides of the affected vertebrae, 35 (87.5%) had granulomas under the anterior longitudinal ligament, 17 (42.5%) had granulomas under the posterior longitudinal ligament, and 1 (2.5%) had psoas abscess; in the 52 patients with advanced diseases, 51 (98.1%) had granulomas on both sides of the affected vertebrae, 49 (94.2%) had granulomas under the anterior longitudinal ligament, 25 (48.1%) had granulomas under the posterior longitudinal ligament, and 4 (7.7%) had psoas abscess; and in the 45 patients in the recovery stage, 34 (75.6%) had granulomas on both sides of the affected vertebrae, 32 (71.1%) had granulomas under the anterior longitudinal ligament, 12 (26.7%) had granulomas under the posterior longitudinal ligament, and 0 (0.0%) had psoas abscess. There was a statistically significant difference in the incidence of granulomas on both sides of the affected vertebrae between the early and advanced stages and between the advanced and recovery stages ($p=0.004$), and there was also a statistically significant difference in the incidence of granulomas under the anterior longitudinal ligament between the advanced and recovery stages ($p=0.060$). In additional, a modern protocol includes DWI, ADC, and post-contrast series could help to ensure an accurate and up-to-date diagnosis of spondylodiscitis.

The performance of different imaging tools in the staging of BS was significantly different. Specifically, the missed diagnosis rate of X-ray was high for BS in the early stage, which was manifested as mild intervertebral space stenosis or no obvious abnormalities; CT was more sensitive to bone destruction (83.9% for advanced stage) and sequestrum; and MRI had better resolution for soft tissue lesions, which was particularly important in the detection of early granuloma (85.4%) and abscess (3.6%). The imaging manifestations of early, advanced, and recovery stages of BS are shown in Figures 2–4, respectively. Imaging features of BS in each stage were systematically summarized (Table 3), and it was found that the combination of CT and MRI had significant advantages in the diagnosis of BS in the advanced and recovery stages (Table 2). Among the 137 BS patients, imaging findings directly altered clinical management in 97 cases (70.8%). For 40 early-stage patients with MRI-detected inflammatory edema but no CT evidence of bone destruction, oral anti-infection therapy was initiated immediately, with treatment timelines shortened by an average of 7.2 days compared to historical controls (who waited for further confirmation). For 52 advanced-stage patients with CT-confirmed bone destruction and MRI-detected paravertebral abscesses, 42 received prolonged intravenous anti-infection therapy (instead of oral therapy) and 10 underwent surgical debridement, with treatment initiation advanced by 4.5 days on

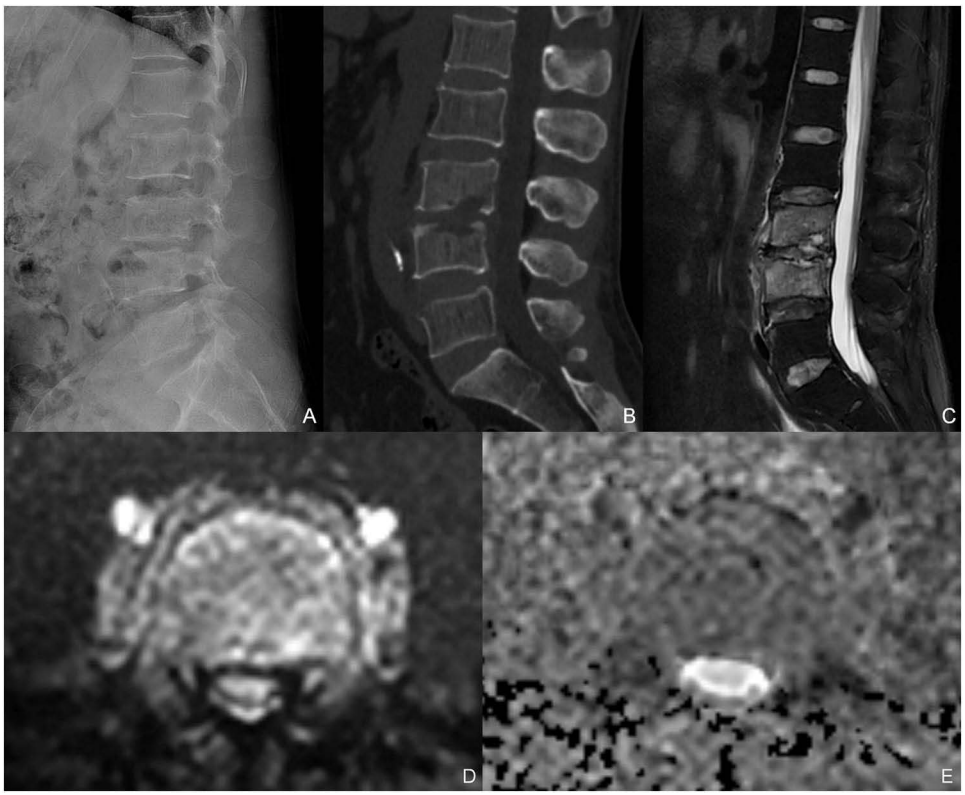

Figure 2 A 46-year-old male was diagnosed with early-stage BS. X-ray diagnosis showed degenerative lumbar bone disease (**A**); sagittal CT scan reconstruction demonstrated bone destruction below the endplate of the lumbar vertebrae 3 and 4, with clear boundaries and no sclerotic edges (**B**); MRI scan with fat-suppressed T2 weighted image (T2WI) sequence showed high signal bone destruction under the endplate of the lumbar vertebrae 3 and 4, and surrounding bone marrow edema (**C**); Axial lumbar Diffusion weighted imaging(DWI) with b-value=600, showing restricted diffusion with hyperintense signal in the paravertebral abscess (**D**); Axial lumbar Apparent Diffusion Coefficient(ADC) map, demonstrating hypointense signal in the abscess with restricted diffusion, with ADC values approximately 0.6–1.0 mm^2/s (**E**).

average to prevent disease progression. Additionally, 5 recovery-stage patients had their treatment courses adjusted (shortened by 2–3 weeks) based on imaging evidence of osteosclerosis.

Discussion

The existing studies on BS imaging have highlighted the diagnostic value of CT and MRI, but most lack systematic analysis of how the diagnostic performance of X-ray, CT, and MRI varies across disease stages.[11,12] The 2023 Chinese Medical Association Consensus on Imaging Diagnosis of Brucellar Spondylodiscitis classified BS into early, advanced, and recovery stages but did not clarify the stage-specific application value of each imaging modality—creating a critical gap in clinical guidance. In this study, we retrospectively analyzed 137 BS patients stratified by the 2023 Consensus criteria, quantitatively comparing the diagnostic strengths of the three modalities across phases (early-stage inflammatory edema, advanced-stage bone destruction/repair, recovery-stage osteosclerosis). Unlike previous study,[10–14] this study integrated X-ray, CT, and MRI data to demonstrate that X-ray misses 90% of early BS but aids in late-stage stenosis detection, CT excels in bone destruction and sequestration identification, and MRI is superior for granulomas and abscesses—especially in advanced stages. Most importantly, we provided novel evidence that CT+MRI synergy improves staging accuracy for early/advanced BS, directly addressing the Consensus' lack of modality combination guidance. These findings offered targeted imaging strategies for different disease phases, supplementing the existing evidence base and enhancing clinical utility for BS diagnosis and treatment planning.

Brucella is a non-encapsulated gram-negative parasitic bacterium, and its pathogenic mechanism is relatively complex. If the antibacterial capacity of the host is weakened, the bacteria will proliferate in the lymph nodes and travel to the whole body along with the blood, and BS may occur after the bacteria reach the spine. Human are generally susceptible to brucella, and the severity of brucellosis is primarily affected by immune status, bacterial virulence and

 https://doi.org/10.2147/JIR.S545126

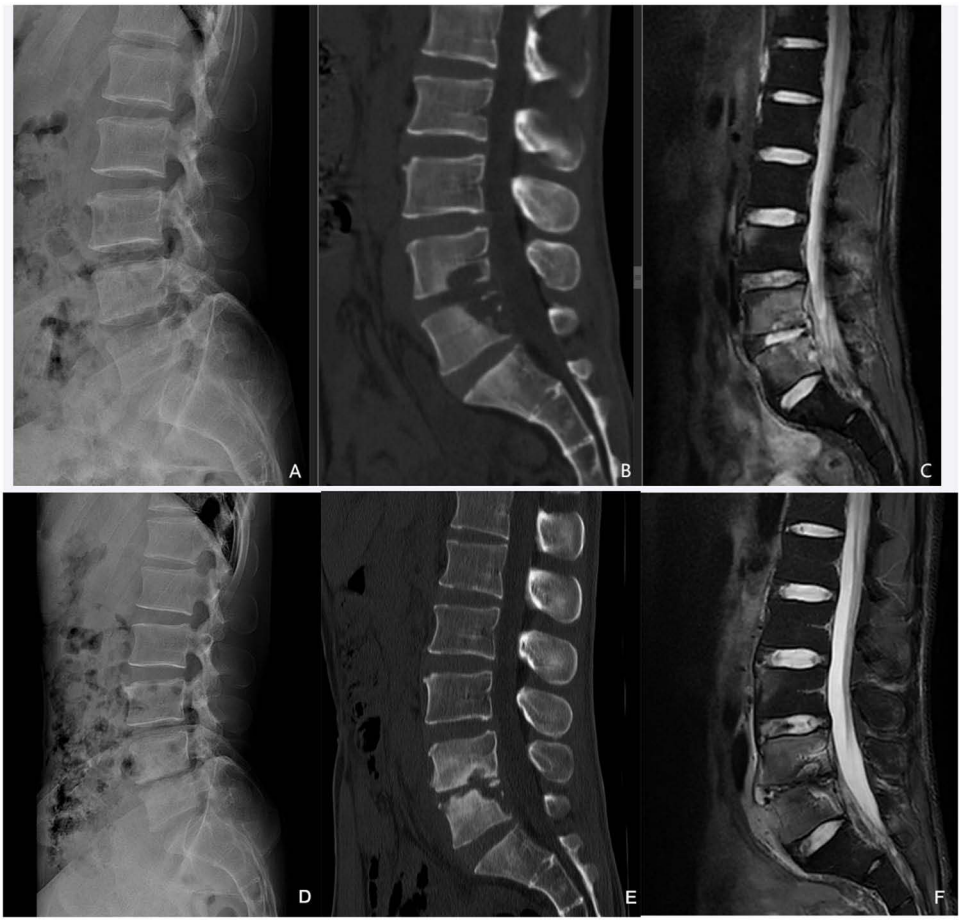

Figure 3 A 35-year-old male was diagnosed with advanced BS. She received antibacterial treatment. Imaging examinations were performed after 7 months. X-ray diagnosis showed degenerative lumbar bone disease (**A**); sagittal CT scan reconstruction demonstrated bone destruction under the endplate of the lumbar vertebrae 4 and 5, with clear boundaries and no sclerotic edges (**B**); MRI scan with fat-suppressed T2 weighted image (T2WI) sequence showed high signal bone destruction under the endplate of lumbar vertebrae 4 and 5, and surrounding bone marrow edema, indicating spondylodiscitis (**C**); Follow-up lateral lumbar X-ray at 7 months after antibiotic therapy showed narrowing of the L4–L5 intervertebral space, slightly reduced bone destruction, and increased sclerotic changes within the affected vertebrae (**D**); Follow-up sagittal CT scan reconstruction of the lumbar spine at 7 months after antibiotic therapy demonstrated narrowing of the L4–L5 intervertebral space, mildly decreased bone destruction, and more extensive sclerotic changes in the affected vertebrae (**E**); Follow-up sagittal T2-weighted MRI of the lumbar spine at 7 months after antibiotic therapy revealed narrowing of the L4–L5 intervertebral space, reduced bone destruction with a distinct low-signal sclerotic rim, decreased bone marrow edema in the affected vertebrae, but slightly increased granulation tissue (hyperintense signal) anterior to the L5 vertebral body (**F**).

infection route. Previous studies have suggested no sex difference in the incidence of brucellosis, and this disease mostly occurs in young and middle-aged population.[10] In the present study, the male to female ratio was 2.68:1, which could be explained by the lumbar strain in men engaged in physical labor.

The diagnosis of BS requires comprehensive epidemiologic, clinical, laboratory and imaging examinations. However, the diagnosis of this disease in comprehensive primary hospitals mainly depends on imaging examination due to the lack of characteristic clinical symptoms and the insufficient use of specific laboratory tests. BS mostly occurs in the lumbar vertebra, followed by the thoracic vertebra and the cervical vertebra. The reason behind may include that the lumbar vertebra is an important load-bearing part of the entire spine and has abundant venous plexus and cancellous bone.[9] Lumbar 3–4, lumbar 4–5 and lumbar 5-sacral 1 among others are most commonly involved. In the present study, the incidence of single-segment involvement is up to 73.7%, which can be explained by the superior endplate rich in blood supply,[13] and the consequent bone destruction of the intervertebral disc and adjacent inferior endplate. The most common involvement site is the lumbar vertebra, with an incidence of up to 98.5%, which was consistent with the findings previous reported.

In imaging diagnosis, X-ray, as an important means of examination, has certain limitations in the diagnosis of BS. In early-stage BS, pathological changes mainly include inflammatory edema and congestion, and bone destruction is

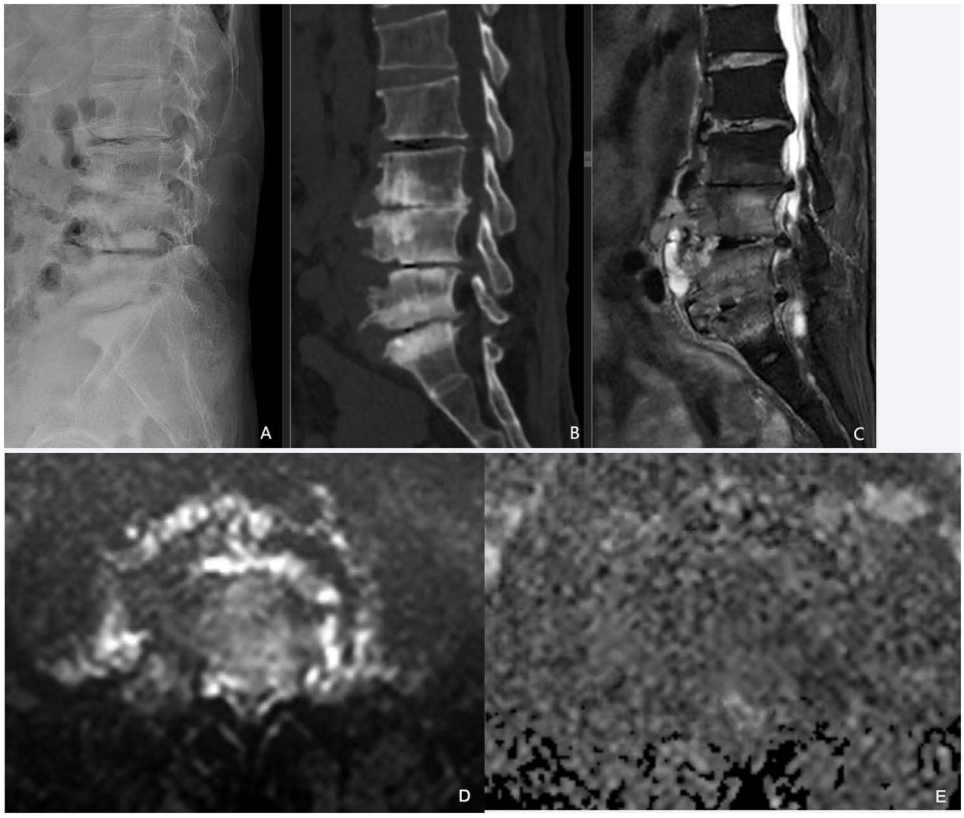

Figure 4 A 58-year-old male was diagnosed with BS in the recovery stage. X-ray diagnosis showed L3-S1 intervertebral space stenosis, and osteosclerosis under the endplate, with no obvious bone destruction (**A**); sagittal CT scan reconstruction demonstrated L3-S1 intervertebral space stenosis, and worm-eaten bone destruction under the endplate (**B**); and MRI scan with fat-suppressed T2WI sequence showed slightly high signal granuloma lesions and high signal microabscess under the anterior longitudinal ligament at the level of L3-S1 (**C**); Axial lumbar DWI (b=600) demonstrated restricted diffusion with hyperintense signal in the paravertebral abscess (**D**); Axial lumbar ADC map showed hypointense signal in the abscess with restricted diffusion, with ADC values approximately 1.2–1.3 mm^2/s (**E**).

relatively mild, Therefore, missed diagnosis of BS is prone to occur during the X-ray examination. In the present study, the overall missed/misdiagnosis rate of early BS with X-ray was as high as 90%. In advanced-stage BS, although bone destruction and disc destruction progressed, the misdiagnosis rate during X-ray examination was close to 10%, and the extent of bone destruction was insufficiently evaluated. In the recovery stage, the missed diagnosis rate of bone destruction under the vertebral endplate was up to 17.5%. This aligns with the findings of Gou et al[12] in 2024, which similarly found that X-rays in early stages only reveal mild intervertebral space narrowing or no significant abnormalities, with a detection rate of less than 15% for pathological changes such as bone marrow oedema and early inflammation. This limitation stems from the requirement for over 30% bone loss to be detectable by X-ray.[14] Early

Table 3 Summary of Imaging Features

Stage	X-ray Features	CT Features	MRI Features
Early	Mild intervertebral space stenosis; no obvious bone destruction	Slightly lower bone density; mild destruction under the endplate; no obvious sequestration	Mainly elevated T2WI signal
Advanced	Significant intervertebral space stenosis; obvious endplate destruction	Intervertebral disc-centered bone destruction; rare sequestration; rare compression fractures	High detection rate of granulomas (85.4%); rare abscesses with high T2WI signal
Recovery	Continuous intervertebral space stenosis; endplate osteosclerosis	Obvious bone repair, and expanded range of osteosclerosis	Attenuated T2WI signal; granulomas still commonly observed

Abbreviations: Advanced CT, Computed Tomography; MRI, Magnetic Resonance Imaging; T2WI, T2-weighted imaging.

https://doi.org/10.2147/JIR.S545126

BS bone destruction predominantly manifests as mild subchondral bone lesions. Furthermore, Fu et al[14] compared imaging features of lumbar fungal versus brucella infections, noting that X-rays may miss mild bone destruction during recovery due to masking by bone sclerosis. The missed diagnosis of early BS can be explained by the small amount of bone destruction in this stage. In the advanced stage, the reason for misdiagnosis included that bone destruction is difficult to observe in the context of intestinal gas interference or lumbar osteoporosis. In the recovery stage, minor bone destruction is difficult to observe due to the overlapping X-ray images, and the interference from extensive osteosclerosis. In the present study, the incidence of vertebral space stenosis on X-ray was higher in the recovery stage than that in the advanced and early stages, which may indicate that the destruction of intervertebral disc gradually worsened if left untreated. Therefore, early diagnosis and treatment are of great significance.

X-ray is still widely used as an initial imaging examination due to its convenience and low cost. However, considering its low sensitivity in the early stage of spondylodiscitis, starting investigations with CT or MRI might be more beneficial for early diagnosis and accurate staging. CT examination has an excellent ability to display mild bone destruction due to its high density resolution, with a high diagnostic value for BS.[15] Particularly, multiplanar reconstruction based on thin-section CT can clearly display mild bone destruction under the endplate, sequestration in bone destruction lesions, and pathological compression fractures of the vertebral body. In the present study, bone destruction was intervertebral disc-centered in all patients with early-stage BS, and the anterior and middle columns of the vertebral body were involved in most cases. Jennin et al[16] indicated that although the detection rate of necrotic bone lesions with a diameter <5 mm in brucellosis-associated spondylitis was low on CT, it was significantly higher than that on MRI (Figure 4A and B). This is in line with the CT detection rate of necrotic bone lesions observed in this study, further supporting the irreplaceable role of CT in assessing bone structural details. In the advanced stage of BS, bone destruction progressed rapidly, and the incidence of sequestration was higher than that in the other two stages, with an overall incidence of about 5%. Compressive fracture after vertebral body destruction caused by BS was rare and compressive fracture and sequestration are relatively rare in BS, providing certain values in the differential diagnosis with spinal tuberculosis and other spinal infectious diseases.[14,17] In early BS, subtle bone destruction can be displayed on CT. In advanced BS, the extent of bone destruction can be comprehensively evaluated using CT multiplanar reconstruction, providing guidance for the placement of screws in surgical patients. In recovery BS, minor bone destruction in the context of extensive osteosclerosis can be observed, with certain value in the outcome observation of disease treatment. Therefore, regardless of the imaging stage of BS, CT scanning is recommended to prevent missed diagnosis and misdiagnosis, and fully evaluate the extent of bone destruction and the treatment effect.

The resolution of MRI for soft tissue is higher than that of CT scan. MRI can clearly show the granuloma and abscess around the affected vertebra. In some studies, the MRI imaging manifestations of BS are classified into three types,[12] including types I, II, and III. Type I corresponds to the early stage, with vertebral bone marrow edema with or without paraspinal edema. Type II corresponds to the advanced stage, and is further divided into types IIa, IIb, and IIc according to the severity of bone destruction in the ventral-dorsal direction of the vertebral endplate. Type III corresponds to the recovery stage, and its subtypes are classified according to the extent of bone destruction and the presence of compression fractures, with no further consideration on perivertebral granuloma. However, we have observed that even in early BS with very mild bone destruction, there is perivertebral granuloma with symptoms of low back pain. With the progression of the disease, the incidence of paravertebral granuloma in the advanced stage of BS is significantly higher than that in the other two stages, and the incidence of granuloma under the longitudinal anterior ligament is also higher in the advanced stage than that in the recovery stage. Even in the recovery stage of BS with bone repair as the main pathology, granulomatous lesions and even abscesses are still present. Therefore, we suggest that MRI is of high diagnostic value in the early, advanced or recovery stage of BS. For patients with obvious low back pain, surgery is a treatment method. The incidence of granuloma under the anterior longitudinal ligament and paravertebral granuloma is higher than that of granuloma under posterior longitudinal ligament. MRI also has certain clinical value in the choice of anterior or posterior approaches. This finding was consistent with the 2020 study by Wu et al[18] on the diagnostic value of ADC in BS, which confirmed that MRI ADC values can quantify the degree of bone marrow oedema. The ADC values in early-stage BS were significantly lower than those in the recovery phase, fully aligning with the trend of ADC value changes observed in this study. Concurrently, research by Yasin et al[19] indicated that combining T2WI signal

characteristics with texture parameters enhances the accuracy of distinguishing BS from pyogenic spondylitis. The features identified in this study – "slightly lower T2WI signal intensity in brucellosis spondylitis granulomas and infrequent abscesses" – may serve as important radiological markers for radiomics analysis, providing a basis for rapid clinical differentiation. MRI diffusion tensor imaging, diffusion imaging and MRI-based radiomics provide additional important imaging methods for the diagnosis and differentiation of BS.[20] Further studies on the application of new MRI technology in BS with different stages are needed.

The imaging features of BS were systematically summarized and the application value of X-ray, CT and MRI in staging of this disease was addressed in the present study. It was found that MRI was particularly important in the identification of early soft tissue lesions, and CT was superior in the detection of bone destruction and dead bone, which was consistent with the findings reported previously.[11] Based on the results of the present study, it is recommended to use CT combined with MRI in clinical practice to reduce missed diagnosis and misdiagnosis, especially in the early and advanced stages of BS, providing patients with guidance for more accurate staging diagnosis and treatment of this disease. Although there are some overlapping imaging features, certain characteristics can aid in differentiation. For example, the presence of paravertebral granulomas and specific patterns of bone destruction might suggest BS rather than other types of spondylitis. Specifically, BS predominantly affects the lumbar spine, typically presenting with worm-eaten-like destruction of vertebral margins accompanied by sclerotic bone proliferation. Narrowing of the intervertebral spaces occurs later and is less pronounced, with ligament calcification and paravertebral abscesses being relatively small. Tuberculous spondylitis predominantly affects the thoracolumbar region, characterised by osteolytic vertebral destruction, marked intervertebral narrowing, and cold abscess formation (often involving multiple vertebrae, extensive in scope, and prone to calcification), which may be accompanied by kyphotic deformity. Pyogenic spondylitis presents acutely, predominantly affecting the lumbar spine. It manifests as early and marked destruction of vertebral endplates with concomitant sclerosis, rapid narrowing of intervertebral spaces, and relatively localised abscesses with infrequent calcification. MRI demonstrates abnormal signals in vertebral bodies and discs for all three conditions. However, tuberculosis frequently forms paravertebral abscesses, Brucellosis abscesses are more localised, and purulent infections commonly present with diffuse bone marrow oedema.

There were limitations in the study. Due to the retrospective and single-center design of this study, potential selection bias may exist and the generalizability of the findings is limited. Moreover, differences in the clinical symptoms, signs, and laboratory tests were not analyzed among patients in different stages. No control group was established for other infectious aetiologies (such as tuberculous or pyogenic spondylitis), differences with other common infectious spondylitis were not further investigated. Although a detailed basis for staging of BS was presented in this study, future case comparison studies with large sample sizes in multiple centers are necessary to further clarify the imaging differences between BS and other diseases. Notably, advanced sequences (eg, DWI/ADC) were not uniformly applied across all cases. This inconsistency may have restricted the ability to explore quantitative imaging markers for BS staging, as these advanced sequences could provide additional pathological insights. Though no significant difference was found in diagnostic accuracy for core features between the contrast/non-contrast subgroups, the lack of contrast in a small subset might have slightly reduced the detectability of subtle enhancing lesions (eg, early abscesses).

Conclusion

Our study comprehensively evaluated the diagnostic performance of X-ray, CT, and MRI in BS across different stages. The results demonstrated that while X-ray has significant limitations in the early detection of BS, CT and MRI offer superior sensitivity and specificity. The combination of CT and MRI provides a comprehensive assessment of both bone and soft tissue involvement, which is crucial for accurate staging and guiding clinical treatment. Based on the limitations of this single-center retrospective study and its preliminary findings, several streamlined directions for future research are proposed: First, multi-center prospective studies with larger sample sizes are recommended to be conducted to verify the the findings of this study across different regions and populations. Second, advanced imaging technologies such as diffusion tensor imaging (DTI), ADC mapping, and radiomics models are suggested to be integrated to develop quantitative imaging markers for BS staging and treatment response evaluation. Furthermore, longitudinal follow-up

studies are proposed to be performed to explore the correlation between imaging indicators and clinical prognosis, thereby providing precise guidance for therapeutic adjustment.

Data Sharing Statement

All data generated or analyzed during this study are included in this published article.

Ethics Approval and Consent to Participate

This study was conducted strictly following the ethical requirements of medical studies in the Helsinki Declaration (2013 Revision) and approved by the Ethics Committee of Kunming Third People's Hospital (Ethical Approval No.: KSLL20230711001-01).

Author Contributions

All authors made a significant contribution to the work reported, whether that is in the conception, study design, execution, acquisition of data, analysis and interpretation, or in all these areas; took part in drafting, revising or critically reviewing the article; gave final approval of the version to be published; have agreed on the journal to which the article has been submitted; and agree to be accountable for all aspects of the work.

Consent for Publication

All participants signed a written informed consent before entering the study. For patients who could not provide written consent (such as minors or under special circumstances), their legal representatives signed on their behalf. Special circumstances include: ① patients who were bed-ridden due to spinal surgery could not sign the informed consent form, which was signed by their legal representatives; ② Some elderly patients in pastoral areas who could not sign the informed consent because of their educational level, which was signed by their legal representatives.

Funding

The study is funded by Science and Technology Program of Kunming City (No. 2024-1-NS-0032) and Scientific Research Foundation of Education Department of Yunnan Province (No. 2024J0882).

Disclosure

The authors report no conflicts of interest in this work.

References

1. Qureshi KA, Parvez A, Fahmy NA, et al. Brucellosis: epidemiology, pathogenesis, diagnosis and treatment-a comprehensive review. *Ann Med*. 2023;55(2):2295398. doi:10.1080/07853890.2023.2295398
2. Mirnejad R, Jazi FM, Mostafaei S, et al. Epidemiology of brucellosis in Iran: a comprehensive systematic review and meta-analysis study. *Microb Pathog*. 2017;109:239–247. doi:10.1016/j.micpath.2017.06.005
3. Tao Z, Chen R, Chen Y, et al. Epidemiological characteristics of human brucellosis - China, 2016-2019. *China CDC Weekly*. 2021;3(6):114–119. doi:10.46234/ccdcw2021.030
4. Liang P, Zhao Y, Zhao J, et al. The spatiotemporal distribution of human brucellosis in mainland China from 2007-2016. *BMC Infect Dis*. 2020;20(1):249. doi:10.1186/s12879-020-4946-7
5. Yang H, Zhang S, Wang T, et al. Epidemiological characteristics and spatiotemporal trend analysis of human brucellosis in China, 1950-2018. *Int J Environ Res Public Health*. 2020;17(7):2382. doi:10.3390/ijerph17072382
6. Yang QJ, Yu BB, Zhang Q, et al. Human brucellosis surveillance and epidemic trend analysisin Yunnan Province from 2010 to 2019. *Chin. J. Zoonoses*. 2023;39(3):258–262. doi:10.3969/j.issn.1002-2694.2023.00.007
7. Jin M, Fan Z, Gao R, et al. Research progress on complications of Brucellosis. *Front Cell Infect Microbiol*. 2023;13:1136674. doi:10.3389/fcimb.2023.1136674
8. Unuvar GK, Kilic AU, Doganay M. Current therapeutic strategy in osteoarticular brucellosis. *North Clin Istanb*. 2019;6(4):415–420. doi:10.14744/nci.2019.05658
9. The joint tuberculosis professional branch of chinese antituberculosis association; the western china bone tuberculosis union; the north china bone tuberculosis union. expert consensus on the diagnosis and treatment of brucella spondylitis. *Chin J Antituberculosis*. 2022;44(6):531–538. doi:10.19982/j.issn.1000-6621.20220138
10. Department of Infectious Diseases. Chinese society of radiology, chinese research hospital society of infection and inflammation radiology professional committee, chinese association of aids prevention and treatment of venereal diseases aids radiology professional committee, et al.

experts consensus on imaging diagnosis of brucella spondylitis. *Chin. J. Med. Imaging Technol*. 2023;39(7):961–965. doi:10.13929/j.issn.1003-3289.2023.07.001.
11. Tu L, Liu X, Gu W, et al. Imaging-assisted diagnosis and characteristics of suspected spinal brucellosis: a retrospective study of 72 cases. *Med Sci Monit*. 2018;24:2647–2654. doi:10.12659/MSM.909288
12. Gou L, Yang Y, Li J, et al. MRI findings and classification of brucella spondylitis: a China multicenter study. *Eur J Med Res*. 2024;29(1):469. doi:10.1186/s40001-024-02011-2
13. Li T, Liu T, Jiang Z, et al. Diagnosing pyogenic, brucella and tuberculous spondylitis using histopathology and MRI: a retrospective study. *Exp Ther Med*. 2016;12(4):2069–2077. doi:10.3892/etm.2016.3602
14. Fu XW, Bi Y, Wei JL, et al. Differences in haematological and imaging features of lumbar spine fungal and brucella infections. *Infect Drug Resist*. 2024;17:4349–4357. doi:10.2147/IDR.S478117
15. Li W, Zhao YH, Liu J, et al. Imaging diagnosis of brucella spondylitis and tuberculous spondylitis. *Zhonghua Yi Xue Za Zhi*. 2018;98(29):2341–2345. doi:10.3760/cma.j.issn.0376-2491.2018.29.013
16. Jennin F, Bousson V, Parlier C, et al. Bony sequestrum: a radiologic review. *Skeletal Radiol*. 2011;40(8):963–975. doi:10.1007/s00256-010-0975-4
17. Guo H, Lan S, He Y, et al. Differentiating brucella spondylitis from tuberculous spondylitis by the conventional MRI and MR T2 mapping: a prospective study. *Eur J Med Res*. 2021;26(1):125. doi:10.1186/s40001-021-00598-4
18. Wu P, Zhang YJ, Guo HB, et al. Values of apparent diffusion coefficient and fractional anisotropy in the diagnosis of brucella spondylitis. *Zhongguo Yi Xue Ke Xue Yuan Xue Bao*. 2020;42(2):154–163. doi:10.3881/j.issn.1000-503X.11300
19. Yasin P, Yimit Y, Abliz D, et al. MRI-based interpretable radiomics nomogram for discrimination between Brucella spondylitis and Pyogenic spondylitis. *Heliyon*. 2023;10(1):e23584. doi:10.1016/j.heliyon.2023.e23584
20. Wu P, Zhang YJ, Qin F, et al. Diffusion tensor imaging in early diagnosis and prognostic prediction of intervertebral disc change in patients with brucella spondylitis. *Zhongguo Yi Xue Ke Xue Yuan Xue Bao*. 2018;40(4):519–527. doi:10.3881/j.issn.1000-503X.10114